Novel acoustic sources from squeezed cavities in car tires

M. J. Gagen
Department of Physics, University of Queensland, Qld 4072, Australia

(Received 10 July 1998; accepted for publication 17 April 1999)

This paper demonstrates that the partial squeezing of car tire cavities at ground impact cannot be adequately modeled by the usual acoustic wave equation. A more complete treatment must begin with the Euler equations for fluid flow in a squeezed cavity to derive a wave equation dependent on cavity wall velocities and accelerations. These can be sizable as ground impact causes the walls of a tire cavity to move with velocities of order 1 m/s and with accelerations of 10^3 m/s^2 over time scales of about 1 ms. Further, the geometry of a typical cavity is such that width compression causes significant increases in pressure and density to occur before the arrival of the rarefaction wave propagating from the open end of the cavity begins to exhaust the full length of the cavity. This causes significant departures from equilibrium density and pressure conditions. These influences are demonstrated both analytically and numerically.
[S0001-4966(99)00708-0]

PACS numbers: 43.50.Lj, 43.25.Ts [MRS]

INTRODUCTION

The loudest component of the far-field noise of cars traveling over 50 km/h and of trucks traveling over 80 km/h is tire noise.[1] Previous treatments examining this area have typically used the low velocities of air movements around the tire/pavement contact point to justify use of the acoustic wave equation and acoustic monopole theory. For instance, monopole theory has long been used to model air pumped from the squeezed cavities in car tires[2] and is well confirmed by experiments showing the dependence of the sound intensity on the second time derivative of volume changes $\ddot{V}$ particularly when the volume changes are simple harmonic. When volume changes depart from being sinusoidal the fit between theory and experiment is not so good.[3] Air pumping noise sources occur as air moves into and out of tire cavities as the tire tread contacts the road and have been modeled by treating the squeezed cavity as an organ pipe with one end closed so as to sustain a $\lambda/4$ resonance. This approach models the air as a piston moving backwards and forwards on a spring.[4–6] Experimental investigations have confirmed the worth of these approaches.[7,8]

Other noise sources include Helmholtz resonances and horn effects between the tire and the road[8,9] as well as from interactions with road pavements[10,11] and bridge grids.[12] Finally, the tire itself possesses certain natural radial and tangential modes of vibration and excitation of these modes generates noise. These modes are usually modeled using variants of circular ring models.[1,13–15]

Jointly, the listed noise sources above are able to explain a significant part of the far-field sound intensity of car tires but cannot be considered a complete explanation. This paper demonstrates that the squeezed cavities in car tires feature large-amplitude pressure and density excursions which lie outside the regime of applicability of small-amplitude acoustic monopole theory and $\lambda/4$ pipe resonance approaches. Rather, we argue that the high accelerations and velocities of the walls of a groove in a car tire can violate the assumptions underlying these approaches. A body of air responds as a damped oscillator to volume changes and pressure differentials[6] and the finite size of the spring constant necessarily means that there is a time delay between a volume change and resulting air movements. In effect, air responds sluggishly to sufficiently fast volume changes. This makes it worthwhile to investigate whether the squeezed cavities of car tires can hit the ground and suffer a volume loss faster than the air within the cavity can evacuate along its length. A typical period over which a cavity undergoes squeezing can be shorter than 0.2 ms and, in this time, a rarefaction wave can only travel about 6 cm. As the lengths of many tire cavities are of this order, it is evident that the volume decrease can occur before the air is able to fully evacuate from the cavity. Then, a decrease in volume by, say, 10% leads to an 11% increase in the density while a 50% volume decrease generates a doubling of the density. These potentially large density fluctuations are well outside the regime of applicability of small-amplitude acoustic theory which explicitly assumes that density and pressure excursions are small. This paper seeks to incorporate the effects of squeezed volume losses within the acoustic wave equation by including cavity wall acceleration and velocity terms.

Some evidence for the plausibility of these claims can be obtained from the literature and this is canvassed in Sec. I. In Sec. II we derive the acoustic wave equation from the Euler equations for adiabatic air flow to examine the underlying acoustic linearization assumptions. We show heuristically in Sec. III that these assumptions are violated in the squeezed cavities of car tires which can generate large pressure and density fluctuations. This motivates us to discard these inapplicable assumptions to give the Euler equations appropriate for squeezed systems in Sec. IV and to rederive a ''squeezed'' acoustic wave equation in Sec. V that contains many sound source terms not included in the usual acoustic wave equation. Subsequently, we discuss approximate analytic solutions to the squeezed Euler equations in Sect. VI and show numerical simulations of a squeezed car tire

groove under typical acceleration and velocity regimes in Sec. VII.

I. EXPERIMENTAL EVIDENCE FOR SQUEEZING EFFECTS

The literature contains some experimental indications that squeezing effects might be important contributions to car tires noise. We canvass this evidence now.

The principle observation implicating squeezing effects in tire noise generation is that of Ejsmont *et al.*[7] where it was noted that there was a nonlinear dependence of emitted sound intensities upon groove width. It was noted that both thin width grooves and large width grooves generate small sound intensities while medium width grooves generate large sound intensities. The width of a groove does not appear in $\lambda/4$ pipe resonance theory which only considers the length of a groove and is not taken into account in monopole theory which only considers time rates of change of the total volume. These observations tend to show that the geometry of a squeezed groove has some influence on sound intensity.

The volume change of a squeezed groove is difficult to observe at high speeds. Estimates of the change in volume range from an assumed 10%[2] to 18% obtained from clay-extrusion measurements.[4] Reference 5 used static measurements to obtain a volume change of 5% and estimated a maximum of 3% at high speeds. These estimates do not take into account the additional loss of volume caused by a bumpy road pavement intruding into the air space of a cavity on ground contact. Typical road pavements might contain gravel fragments of 5 to 8 mm in size which is similar to the groove widths of a typical tire cavity[8] so these gravel fragments might routinely cause additional volume losses greater than those estimated above. It has been well established that the far-field sound intensity depends on highly nonlinear interactions between a tire tread and road pavements with, for example, observations that certain surfaces may be relatively noisy for cars but silent for trucks.[10,16]

These volume deformations occur as the groove moves into contact with the ground at which point the tire wall is subject to radial accelerations of up to 3300 m/s^2 peak to peak and tangential accelerations of about 1000 m/s^2 peak to peak on millisecond timescales. These accelerations are typical of a car traveling at 80 km/h[1,8] and it is these accelerations which cause the volume loss on time scales faster than the air can evacuate from the cavity.

II. ACOUSTIC THEORY

The usual acoustic wave equation is derived in the low velocity and adiabatic limits of the Euler equations for fluid flow. The conservative form of the inviscid and dimensionless Euler equations in two dimensions for perfect gases in the adiabatic limit and with zero conductivity are[17–21]

$$\partial_t U+\partial_x F+\partial_y G=0,$$

$$U=\begin{pmatrix}\rho\\ \rho v_x\\ \rho v_y\end{pmatrix},\quad F=\begin{pmatrix}\rho v_x\\ \rho v_x^2+\rho^\gamma/\gamma\\ \rho v_x v_y\end{pmatrix},\quad G=\begin{pmatrix}\rho v_y\\ \rho v_x v_y\\ \rho v_y^2+\rho^\gamma/\gamma\end{pmatrix}. \tag{1}$$

Here, we show the mass continuity (top line) and momentum conservation equations in the x and y directions with velocities v_x and v_y, respectively. (We exploit symmetry to constrain fluid motions to this plane.) The adiabatic limit is realized by relating fluid pressure p to fluid density ρ as $p=\rho^\gamma$ where $\gamma=1.4$ is the usual ratio of specific heats. All variables are dimensionless with dimensioned (primed) variables being given by $x'=xL$, $v'=va_0$, $p'=pp_0$, $\rho'=\rho\rho_0$, and $t'=tL/a_0$ with L being some convenient length parameter and $a_0^2=\gamma p_0/\rho_0$ being the local speed of sound in ambient pressure and density conditions of p_0 and ρ_0. With these choices a unit velocity equates to the speed of sound in the fluid.

The appearance and propagation of acoustic disturbances is entirely described by Eq. (1) but is usually written as a wave equation[21] after making the small wave approximation. In nondimensional units, a Taylor series expansion in pressure gives

$$p=1+p_1 \tag{2}$$

and

$$\rho=1+\left.\frac{\partial\rho}{\partial p}\right|_0(p-1)+\left.\frac{\partial^2\rho}{\partial p^2}\right|_0\frac{(p-1)^2}{2}$$

$$=1+p_1/\gamma+\frac{1}{2\gamma}\left(\frac{1}{\gamma}-1\right)p_1^2. \tag{3}$$

This Taylor expansion is valid only when $p_1\ll 1$ and we can truncate the expansion at the first term to give small-amplitude acoustic theory. (The error involved in this truncation equates to the second term and is non-negligible when pressure fluctuations are greater than about $p_1>10^{-2}$. In this paper we will show that squeezed systems generate densities of $\rho=1.1$ in dimensionless terms, giving $p_1\approx 0.14$ with a resulting truncation error of 0.002 which cannot be ignored.)

The acoustic wave equation is then obtained by differentiating Eq. (1) or its three-dimensional equivalent to solve for $\partial_{tt}\rho$ with the further assumption of small fluid velocities $v_x, v_y\ll 1$ to give

$$\partial_{tt}p_1-\partial_{xx}p_1-\partial_{yy}p_1-\partial_{zz}p_1=0, \tag{4}$$

where now we explicitly show the third dimension to permit comparisons to the derivations below.

Acoustic monopole theory applies this equation to a vibrating point source modeled as a small spherical emitter of radius R undergoing small oscillations much less than the radius $\dot{R}\delta t\ll R$. The resulting volume changes are then $\dot{V}=4\pi R^2\dot{R}$ which cause spherically symmetric pressure waves to propagate into the surrounding medium. These pressure waves decay as $1/r$ and have the usual functional dependence on $(r-a_0t)$ to satisfy the wave equation and to describe delayed waves traveling outwards from the sphere at speed a_0. Thus, at the point (r,t), the pressure has functional dependence

$$p_1(r,t) \propto \frac{\overline{p}(r-a_0 t)}{r}. \tag{5}$$

In spherical coordinates with approximately constant fluid density the conservation of momentum equation (1) is $\rho \partial_t v_r = -\partial_r p_1/\gamma$ where we set $v_r^2 = 0$ for low fluid velocities. Substituting Eq. (5) here gives

$$\rho \partial_t v_r \propto -\partial_r \frac{\overline{p}(r-a_0 t)}{\gamma r} \propto \frac{\overline{p}}{\gamma r^2} - \frac{\partial_r \overline{p}}{\gamma r}. \tag{6}$$

This solution applies at the surface of the sphere where $r = R$ is small and assumed to be much smaller than the wavelength of sound emitted, allowing us to ignore the second term on the rhs. Noting that $v_r = \dot{R}$ and $\ddot{R} \approx \ddot{V}/(4\pi R^2)$ we have

$$\frac{\rho \ddot{V}}{4\pi R^2} \approx \frac{\overline{p}}{\gamma R^2}. \tag{7}$$

In turn, this allows us to solve for $\overline{p}$ and to substitute this back into Eq. (5) to obtain

$$p_1(r,t) \approx \frac{\gamma \rho \ddot{V}}{4\pi r} \tag{8}$$

relating the pressure wave emitted by a monopole source to the second derivative of the volume change of that source. Dipole and quadropole sources are then constructed from appropriate arrays of monopoles.[21]

Demonstrations of the failure of monopole theory can be easily derived when we consider a small spherical balloon attached by a thin straw to a pump so that its volume can be changed in a controlled manner. We consider two cases where the small balloon undergoes a linear collapse to zero volume with constant acceleration $\ddot{V} = 0$ and where the balloon undergoes a collapse and rebound sequence obtained by setting $\ddot{V} = c$, a positive constant, to obtain a volume quadratic in time.

The linear collapse of the balloon described by $\ddot{V} = 0$ gives volume $V(t) = V_0(1 - t/T)$ for suitable constants V_0 and T and is expected to produce a rarefaction wave in the surrounding medium which should be heard if severe enough. However, this pressure fluctuation makes no appearance in monopole theory which predicts a pressure fluctuation of zero.

Simple experiments can be performed to confirm the inadequacy of the monopole predictions. Clapping your hands together features linear squeezing with $\ddot{V} = 0$ except at the time of impact so monopole theory predicts no sound emission at all prior to this time and claims that the ''clap'' comes only from the instantaneous decelerations and body vibrations caused by impact. This prediction can be shown to be incorrect by first clapping your hands with the fingers together and then clapping with the fingers spread apart. By use of two experiments we create a control which allows us to eliminate the deceleration from consideration as both experiments feature the same decelerations and body vibrations. (The position of the fingers will not change decelerations or vibrations.) The very different magnitudes of the claps generated in these two experiments arising from exactly the same decelerations means sound intensities cannot be entirely explained by monopole theory with its exclusive reliance on volume accelerations as a source of noise.

A clearer failure occurs when we consider a balloon underdoing a volume acceleration $\ddot{V} = c$, a positive constant, to give a volume varying quadratically in time as $V(t) = (V_0 - \delta V)(1 - t/\tau)^2 + \delta V$ where V_0 is the initial volume and δV is the small volume of the balloon at the time τ of smallest radius. Here, the collapse and rebound of the balloon is expected to produce first a rarefaction wave followed by an overpressure wave which should be heard if the movements are severe enough. However, monopole theory predicts an always positive constant pressure wave $p_1 \propto 2(V_0 - \delta V)/\tau^2$.

Monopole theory has a restricted domain of applicability due to the very simplicity which is its principle advantage. As mentioned previously, air responds sluggishly even to local volume changes as a damped oscillator while monopole theory equates local air movements exactly with the volume changes of the system. (This sluggishness is additional to the usual propagation delays of wave motion at finite speed.) Further, simple source monopole theory considers only single frequency, simple harmonic motions.[21] For motions which are not simple harmonic, we should first perform a Fourier decomposition into frequency components before applying monopole theory. When volume changes are linear or quadratic the Fourier decomposition is broad and acoustic emissions are not well modeled by single-frequency monopole theory. We note that Fig. 14 of Ref. 3 shows that monopole theory correctly predicts acoustic intensities when volume changes are approximately simple harmonic and provides poor predictions otherwise.

Any treatment of volumes varying linearly and quadratically in time requires a rederivation of the acoustic wave equation properly taking account of the geometry of the system and allowing for the velocity and acceleration of the groove walls. We heuristically motivate a full examination of such systems in the next section.

III. PRESSURE AND DENSITY FLUCTUATIONS IN TIRE GROOVES

We seek to heuristically consider density (and pressure) fluctuations in a tire groove undergoing squeezing as it enters the contact patch.

Consider a tire traveling forward at linear speed v with a groove etched into its rim that is orientated at angle ϕ to the direction of travel, and suppose that the groove, initially of width d_0, undergoes a compression to width d_1 as it enters the tire–road contact patch. The groove is expected to compress as the surrounding rubber takes the full weight of the vehicle. This situation is shown in Fig. 1. It seems reasonable to assume that the groove is subject to an inflow of air along its length as the rubber side walls (hatched areas) descend onto the road and displace air sideways. This implies that the pressure wave caused by squeezing will dissipate only after the wave has traveled the full length L of the groove.

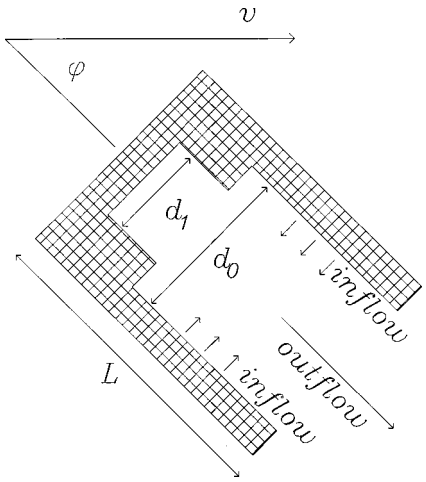

FIG. 1. Squeezed geometry for tire grooves orientated at angle ϕ to the direction of travel.

(Throughout we consider a groove with one end closed—the analysis can be applied to an open ended groove of twice the length.)

The groove of length L has projection $L\cos\phi$ in the direction of travel and undergoes a squeezing along its entire length L in time $L\cos\phi/v$. The compression point on the groove then has velocity of

$$v_c=\frac{v}{\cos\phi}. \tag{9}$$

The groove squeezing causes an increase in the density and pressure of the cavity which propagates to the end of the cavity at the sound speed a_0 (for small fluctuations). To a first approximation, air cannot leave the cavity until this pressure wave has traversed the full length of the cavity which takes a time $\tau=L/a_0$. In this same time the cavity has undergone a volume decrease $\delta V=(d_0-d_1)v_c\tau W$ from its intial volume $V_0=d_0LW$. As no air has escaped to time τ we can immediately write the average density at time τ as

$$\rho=\frac{\rho_0V_0}{V_0-\delta V}, \tag{10}$$

where ρ_0 is the initial density in the groove. In dimensionless terms, the density fluctuation $\delta\rho=(\rho-\rho_0)/\rho_0$ is

$$\delta\rho=\left[\frac{d_0a_0\cos\phi}{(d_0-d_1)v}-1\right]^{-1}. \tag{11}$$

As shown previously, we can ignore pressure and density fluctuations when these fluctuations are small and less than of order 10^{-2}. Conversely, we cannot ignore squeezing effects when $\delta\rho>10^{-2}$ or when

$$\frac{d_0a_0\cos\phi}{(d_0-d_1)v}<10^2. \tag{12}$$

Noting $a_0\approx340$ m/s and typical squeezing volume losses of around $d_0/(d_0-d_1)\approx10$ gives

$$\frac{\cos\phi}{v}<0.03 \tag{13}$$

to indicate when squeezing effects cannot be ignored.

In practical terms, when the forward speed of the car is $v=100$ km/h or $v=28$ m/s we find that all grooves of orientation angle $\phi>33$ degrees will undergo significant fluctuations due to squeezing. Conversely, if grooves are oriented at angles of $\phi=45$ degrees say, then squeezing effects are relevant only above speeds of $v=24$ m/s or $v=85$ km/h. This is precisely the speed range at which unexplained tire noise occurs.

The simple heuristic treatment of this section demonstrates that squeezing effects are expected to cause significant departures from ambiant pressure and density conditions with the magnitude of these departures invalidating the usual first-order Taylor series truncated acoustic theory. A proper analysis of a compression point moving along a groove at arbitrary angle ϕ is difficult and would require spatial- and time-dependent coordinate transforms. This lies outside the scope of this paper. However, by narrowing our focus to consider only squeezed grooves orientated perpendicularly to the direction of travel, we are able to model squeezing effects using only time-dependent coordinate transformations and this is feasible. We turn to consider these methods now.

IV. FLUID DYNAMICS IN SQUEEZED CAVITIES

Most fluid dynamical flow problems are solved in regions defined by stationary boundaries. In contrast, we consider a region with dynamic boundaries chosen to change the nature of the solutions of the system of fluid equations. In effect, the boundary dynamics are described by their own boundary equations which are additional to the usual fluid equations. It is well understood that adding further equations to a given system of equations will usually change the nature of the solution space. A common example of how moving boundaries can modify the acoustic field within a region is the active control of noise in vehicles.[22] Here, loud speakers are used to pump out-of-phase sound across the boundary of the vehicle to cancel pressure fluctuations within that vehicle. Then, the moving boundary ideally forces the solution of the acoustic wave equation to be one of constant density $\rho=1$ and constant pressure $p=1$ everywhere in the vehicle. However, active control approaches typically deal only with small amplitude acoustic waves and boundary movements which are small compared to the size of the vehicle. In this paper we consider large pressure and density excursions which cannot be treated using small wave acoustic theory.

Consider the fluid in a region contracting due to external applied forces as shown in Fig. 2. Here a board of length L is

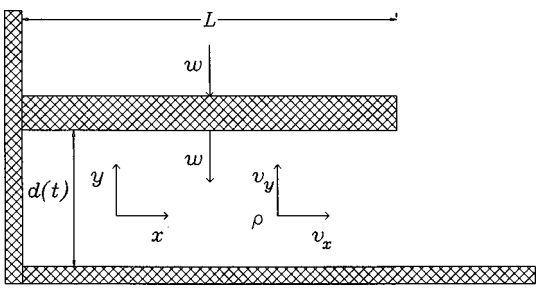

FIG. 2. Squeezed geometry for tire grooves orientated perpendicular to the direction of travel.

descending at velocity w towards a surface. The enclosed fluid is moving with velocity (v_x, v_y) and is expected to be ejected from between the boards into the outside uncompressed region as the internal pressure builds up. (We exploit symmetry to ignore the z direction.) We model the separation distance as $d(t)=d_0 f(t)$ with time-dependent function chosen so that $f(0)=1$ and $w=d_0\dot{f}$.

This system is entirely described by the Euler equations (1) together with dynamical boundary conditions specifying that the fluid velocity is constrained to have $v_y=w$ along the top and bottom surfaces of the descending board and to have $v_x=0$ on the right-most vertical edge of the board. (Here we consider an inviscid fluid.) An entirely identical description of this squeezed physical system can be obtained by making a time-dependent coordinate transformation[19]

$$x=x, \quad y=f(t)\chi+g(t), \quad t=t \tag{14}$$

designed to render the moving board stationary mathematically. This is achieved by choosing $f(t)$ and $g(t)$ so that as the board in real space changes its y position, the functions f and g are varied so as to leave the χ position of the board constant in computational space.

To clarify the physical meaning of this dynamic coordinate transformation consider the case where the board is descending smoothly at constant speed w, and for simplicity consider regions where $g(t)=0$ (the compressed region between the boards). Then, air parcels immediately adjacent to the descending board must have vertical velocity $w=\dot{f}<0$, while air located adjacent to the stationary bottom surface must have zero vertical velocity. Further, for small speeds w it is reasonable to expect that the the air parcels located half way between the descending board and the stationary bottom surface will have vertical speeds of $w/2$ and, in general, that the vertical air speed is linearly proportional to the relative height of an air parcel between the stationary surface and the descending board. This linear velocity dependence (valid only at slow speeds) is realized by having air located initially at height y_0 (where the maximum height is set to unity) moving downwards in physical space with velocity $v_y=y_0\dot{f}$. The initial height at time $t=0$ when $f(0)=1$ satisfies $y_0=\chi$ in Eq. (14) giving $v_y=\dot{f}\chi$ with different χ for different parcels of air. A linear dependence of vertical velocity on initial height is achieved by setting $v_y=\dot{f}\chi$, or as it is convenient to define the parameter $v_\chi=(v_y-\dot{f}\chi-\dot{g})/f$ and we achieve a linear dependence of the vertical velocity on initial height by setting $v_\chi=0$.

Standard change of coordinate methods[23] or consultation of the helpful Ref. 19 then give the computational space fluid equations as

$$\partial_t U+\partial_x F+\partial_\chi G=0,$$

$$U=\begin{pmatrix} f\rho \\ f\rho v_x \\ f\rho v_y \end{pmatrix}, \quad F=\begin{pmatrix} f\rho v_x \\ f(\rho v_x^2+\rho^{\gamma}/\gamma) \\ f\rho v_x v_y \end{pmatrix}, \tag{15}$$

$$G=\begin{pmatrix} f\rho v_\chi \\ f\rho v_x v_\chi \\ f\rho v_y v_\chi+\rho^{\gamma}/\gamma \end{pmatrix}.$$

Here, we mix terms v_y and $v_\chi=(v_y-\dot{f}\chi-\dot{g})/f$ to maximally simplify the equations. These equations reduce to the usual Euler equations (1) in the limit $f=1$, $g=0$, and $y=\chi$.

In real space, the squeezing of the boards compresses the inside air to expel a jet of air while in computational space the board is stationary. Here, squeezing forces have been converted into mass and momentum injection terms proportional to $\dot{f}/f$ with the injection of mass and momentum everywhere into the space between the boards generating the observed jet of air in exactly the same way as a solid-fuel rocket.[17,18] This indicates that whenever we have large wall velocities, $\dot{f}\approx 1$ in dimensionless units, we can expect significant expelled jet flows.

V. SQUEEZED ACOUSTIC WAVE EQUATION

That squeezed systems can violate the assumptions underlying monopole theory in at least two regimes is made apparent by solving for $\partial_{tt}\rho$ using the squeezed fluid equations (15) without making the small wave or low-velocity approximations. The squeezed wave equation with all terms is

$$\begin{aligned} 0=\partial_{tt}\rho-\frac{\partial_{xx}\rho^{\gamma}}{\gamma}-\frac{\partial_{\chi\chi}\rho^{\gamma}}{\gamma f^2}-\partial_{xx}(\rho v_x^2)-\partial_{x\chi}(\rho v_x v_\chi) \\ -\frac{\partial_{\chi x}(\rho v_x v_y)}{f}-\frac{\partial_{\chi\chi}(\rho v_y v_\chi)}{f}+\frac{\ddot{f}}{f}\rho+\frac{2\dot{f}\partial_t\rho}{f} \\ -\frac{\partial_{\chi t}[\rho(\dot{f}\chi+\dot{g})]}{f}-\frac{\dot{f}\partial_\chi(\rho v_y)}{f^2}. \end{aligned} \tag{16}$$

This equation reduces to the usual small amplitude wave equation (4) in the limits $f=1$, $g=0$, v_x, $v_y\ll 1$, $p=1+p_1$ for $p_1\ll 1$, and $\rho=1+p_1/\gamma$.

Here, it is apparent that terms previously left out in the usual wave equation treatment become large in either of two limits. The first is at full closure with $f\to 0$ and $\dot{f}\neq 0$. This case shows a finite-time singularity in the fluid dynamics which places a regular singular point into the fluid equations. Regular singular points in dynamical equations can have the effect of driving solutions to exhibit singularities, and, in other work, we explore how these singularities can drive supersonic expelled jets from squeezed systems[24] and relativistic jets from large astrophysical systems. However, cavities in car tires are not usually squeezed to a singularity and generally have $f\approx 1$.

The second case of interest occurs in the limit of high wall velocities and accelerations when $O(\dot{f})\approx O(\dot{\rho})$ or $O(\ddot{f})\approx O(\ddot{\rho})$. Car tires can approach these regimes.

Consider a typical groove of length $L=7.5$ cm, width $d_0=5$ mm, and depth $W=d_0$ cut into the rim of a tire traveling forward with linear speed v. As the groove moves into the contact patch with the road (to take the full weight of the car) the groove undergoes a squeezing of its volume of around 10% modeled by a compression of the width of $A=0.1d_0=0.5$ mm. The groove uncompresses a time τ_c

$=d_c/v$ later when it leaves the contact patch of length about $d_c=20$ cm. Groove squeezing occurs in a time $\tau\approx d_0/v \approx 0.3$ ms at $v=15$ m/s or about 50 km/h.

Simple estimates of the velocity and acceleration of the groove wall are then $\dot{d}\approx A/\tau\approx 1.5$ m/s and $\ddot{d}\approx A/\tau^2 \approx 4500\,\text{m/s}^2$. These calculations are in accord with observation.[1,8] In this paper, the width of groove is modeled by $d(t)=d_0 f(t)$ so, in nondimensional units, we have

$$\dot{f}=\frac{\dot{d}}{d_0}=\frac{ALv}{a_0 d_0^2}, \quad \ddot{f}=\frac{\ddot{d}}{d_0}=\frac{AL^2v^2}{a_0^2 d_0^3}. \tag{17}$$

We note that the dimensionless acceleration increases quadratically with linear speed v. These simple estimates give $\dot{f}\approx\ddot{f}\approx 0.1$ at $v=25$ m/s, or about 90 km/h, and increasing at higher speeds. These values are compared to $\rho\approx 1$ in dimensionless units, indicating that squeezing can have significant effects on fluid dynamics.

VI. ANALYTIC SOLUTIONS TO SQUEEZED SYSTEMS

In this section we briefly provide indicative solutions for the fluid flow in squeezed systems as we seek to understand the nature of the expelled jet including how its kinetic energy might eventually contribute to the far-field sound intensity via turbulence or vortex generation.

A physical understanding of a squeezed system of Fig. 2 is readily had by considering a constant density approximation which allows equating the loss of internal volume $\delta V = -LWw\,\delta t$ with the gain in volume of the expelled jet $\delta V = Wd(t)v(L,t)\,\delta t$ giving

$$v(L,t)=-\frac{wL}{d(t)}=-\frac{\dot{f}L}{f}. \tag{18}$$

As mentioned previously, simple experiments confirm the importance of the spatial amplification factor L: clap your hands with fingers together ($L\approx 3$ cm) and with fingers apart ($L'=L/4$) noting the different sounds.

Two particular analytic solutions of interest can be obtained for linear squeezing $f(t)=1-t/T$, $\dot{f}=-1/T$, and with $g=0$. Here, T is the closure time of the cavity. We further assume smoothed vertical flows $\partial_\chi\rho=0$, $v_\chi=0$, and $v_y=\dot{f}y$.

The first solution of interest is a squeezed cavity with both ends closed—a piston—obtained by setting all x gradients and v_x equal to zero. This reduces Eq. (15) to $\partial_t(f\rho)=0$ with nondimensional solution

$$\rho(t)=\frac{1}{f}. \tag{19}$$

Here we see that a linear squeezing of 10% immediately generates a commensurate increase in density.

The second solution applies to an open ended cavity with nonzero x gradients and velocities $v_x\neq 0$. We still consider expulsion velocities small enough to satisfy $v_x^2=0$. If we then assume approximately constant density $\rho=1$, then both Eqs. (1) and (15) are satisfied by

$$v_x(x,t)=-\frac{\dot{f}x}{f}, \tag{20}$$

which extends the previous heuristic solution of Eq. (18). This solution is strictly valid only while $v_x<0.3$ where free-flowing air remains approximately uncompressed, but this is expected to be satisfied for car tires.

In time δt, a mass $\delta m=\rho LWd_0\dot{f}\,\delta t$ is expelled at velocity $v(L,t)$ given by Eq. (20) and with kinetic energy $\delta E=(\frac{1}{2})\delta m v^2$. This integrates to give total mass expulsion to time t of

$$m(t)=m_0(1-f) \tag{21}$$

and total kinetic energy of the expelled jet of

$$E(t)=-E_pT^2\int_0^t dt(\dot{f}^3/f^2), \tag{22}$$

where $m_0=\rho LWd_0$ is the initial fluid mass and $E_p=\frac{1}{2}m_0(L/T)^2$ is the kinetic energy of a mass m_0 moving over distance L in closure time T. For the constant-velocity linear squeezing case with loss of volume given by $\delta V/V=t/T=A/d_0$ this gives

$$m=\frac{A}{d_0}m_0, \quad E=\frac{A}{d_0-A}E_p. \tag{23}$$

This last relationship gives the kinetic energy of the jet as proportional to the square of the velocity of the car as

$$E=\frac{\rho WA^3L^3v^2}{2(1-A/d_0)d_0^4}. \tag{24}$$

The velocity solution of Eq. (20) can also be used to suggest the evolution of spatial density concentrations along the length of the expelled jet. Consider a jet with expulsion velocity given by Eq. (20) so that at the open end of the cavity where $x=L$ the horizontal velocity at time t is $v_x(L,t)=-\dot{f}L/f(t)$. We note the velocity of air parcels expelled at different times is different though once any air parcel has escaped from the cavity it is no longer compressed or accelerated (to a first-order approximation). This allows applying a constant velocity approximation to motion outside the cavity to give an estimate of the position of any particular air parcel at later times. Then, the position at closure time T of a particle expelled at the earlier time t is

$$X(t,T)=L+v(L,t)(T-t). \tag{25}$$

For linear squeezing we have $f(t)=(1-t/T)$ giving $X(t,T)=2L$ for all the expelled particles in the air jet, implying an approximate density distribution of

$$\rho(x,T)\propto\delta[x-2L]. \tag{26}$$

Such density concentrations, if large enough, can source the formation of shock fronts within the jet and can contribute to far-field sound intensities.

The above discussions can contribute to understanding sound sources from squeezed cavities in car tires. For instance, the assumption that the velocity of the expelled jet causes turbulence to generate sound waves suggests that the sound intensity will depend on the ratio L/d, or the geometry

of the cavity. This is in accord with observations that both thin width and large width grooves emit less sound than medium width grooves.[7] Evidently, for large grooves $L \approx d$ and velocities are small so no sound from air jets is expected. Medium width grooves have $L > d > 0$, giving a ratio L/d large enough to give significant sound emission. Finally, thin width grooves with $d \approx 0$ have very little air in them so the initial mass $m_0 \approx 0$, meaning that the kinetic energy of the expelled jet is never significant and little sound is expected.

It is beyond the scope of this paper to discuss extreme nonlinearities like the formation of shock fronts in expelled jets, and our inviscid treatment means that we cannot comment about the sound generation role, if any, of vortices in the expelled jet.

VII. NUMERICAL SIMULATIONS

Squeezed cavities are analytically intractable and necessitate a resort to computational fluid dynamics (CFD) and we apply MacCormack's technique to Eq. (15). This standard scheme employs an explicit finite element method which is second order accurate in space and time.[20,25]

Consider a tire moving at approximate speed $v = 25\,\text{m/s}$ with grooves of length $L = 7.5\,\text{cm}$ and width and depth $d_0 = W = 5\,\text{mm}$. The groove undergoes a compression of 10% over a time of about 0.2 ms.

We note that in this time a rarefaction wave can only just travel from the open end of the groove to the closed end of the groove ($L \approx a_0 \tau \approx 6\,\text{cm}$) where pressure and density is building up. Further, sound waves have made about 15 crossings of the width of the groove to equilibrate the pressure and density across the width. Before the arrival of the rarefaction wave at any point, the fluid gradients in the x direction are zero and the piston solution of Eq. (19) is applicable. Thus, we expect that a 10% squeezing of the groove will cause a roughly 11% increase in density near the closed end of the groove. The arrival of the rarefaction wave will then cause a density gradient of about 11% between the closed and open ends of the groove and this gradient will generate velocity gradients of order 0.11 in the x direction leading to expulsion velocities of $v_x \approx 0.11$ at the open end of the cavity. This translates into speeds of about 30 m/s. These simple expectations are met in the simulations below.

The CFD numerical simulation is shown in Fig. 3 which shows the groove walls as the raised sections of the graph. (Only the top edge of the groove is shown for clarity.) The top edge is stationary in computation space but has caused a 4% compression in graph (a) and a 10% compression in graph (b). In graph (a) we see that the compression has equilibrated across the narrow width of the cavity and the density has increased by about 4% in accordance with Eq. (19). The increase in density causes a rarefaction wave to propagate from the open end of the cavity to the left but this wave has only had time to move a limited distance along the cavity. In graph (b) we reach the full compression of 10%, causing the density to increase by approximately 11%. This is also the time at which the rarefaction wave reaches the end of the cavity and all the air begins to exhaust from the cavity.

As previously noted after Eq. (3), a density fluctuation of 11% corresponds to a pressure fluctuation of 14% and the magnitude of this fluctuation lies well outside the validity regime for a linear truncation of the Taylor series expansion underlying small amplitude acoustic theory. It is for this reason that we must use the full Euler equations to derive the squeezed wave equation (16).

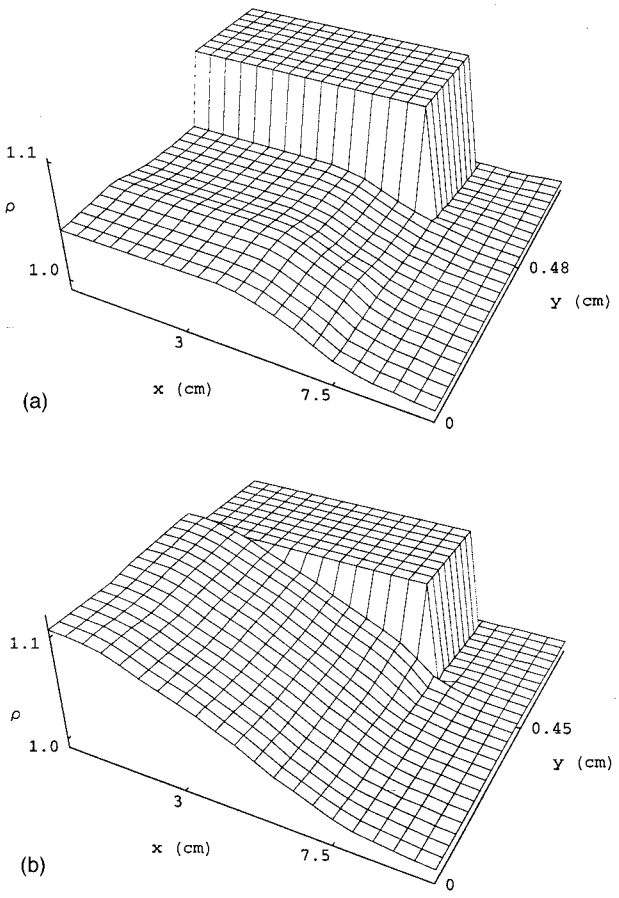

FIG. 3. The density profile of the air contained within the squeezed cavity (with only top wall shown) at times $t = 0.05$ ms with 4% squeezing in graph (a) and at $t = 0.2$ ms with 10% squeezing in graph (b). The density is given in dimensionless units. (Note the changes in the vertical scale as the groove compresses.)

Once the air begins to evacuate, the piston solution is no longer valid and we must consider the velocity solution of Eq. (20) with its linear dependence on position x. The validity of this solution is shown in Fig. 4 at the time of 10% squeezing which clearly shows the expected linear increase of velocity with position. This also confirms our simple ex-

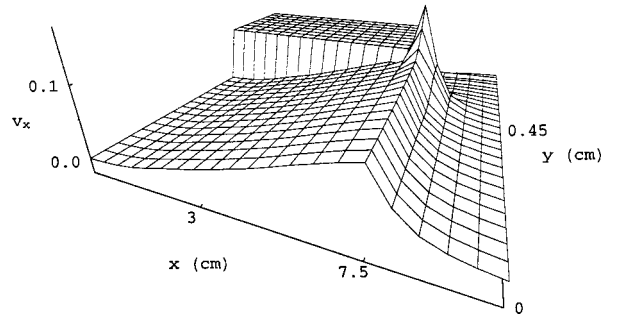

FIG. 4. The linear dependence of expulsion velocity on position x in dimensionless units.

pectation of a maximum velocity of around $v_x \approx 0.1$ in dimensionless units at the open end of the tube.

It is expected that the observed velocity flows will exhaust the cavity back to atmospheric pressure over the 6-ms period during which the cavity passes through the contact patch between the tire and the road. Then, the cavity will uncompress by about 10%, causing a decrease in density and pressure below ambient conditions by about 10%. The cavity will then open along its length and the pressure and density fluctuations are then expected to drive Helmoltz and Horn resonances.

These simulations serve to confirm the relevance of the analytic solutions for density under piston conditions in Eq. (19) and for the expulsion velocity in Eq. (20). However, they do not give insight into the far-field sound intensity emitted from squeezed cavities as the numerical grid is to coarse by a factor of 10 or more while a full simulation of passage through the contact patch (taking about 6 ms) requires an increase in grid area by a factor of 30^2. Thus, a full simulation is about 90 000 times larger than that shown here and is computationally intractable at this time.

VIII. CONCLUSION

In this paper we derived a squeezed acoustic wave equation suitable for application to squeezed fluid systems. The starting point of this derivation was the Euler equations for fluid flow together with the moving boundary conditions specifying a cavity under compression. This derivation demonstrated that the usual assumption of a small-amplitude acoustic wave equation and the acoustic monopole theory derived from this equation is incorrect for squeezed systems.

Approximate analytic solutions were obtained for the fluid flow in squeezed systems and were used to identify a pistonlike increase in density within a squeezed cavity before the cavity begins to exhaust along its full length. These solutions show that the exhaust velocity has a linear dependence on cavity length and can reach significant speeds. The mass and kinetic energy and density structure of the resulting expelled jet were examined using the derived approximate solutions. Finally, we used computational fluid dynamics approaches to directly investigate fluid flow and to confirm the applicability of the approximate analytic solutions.

ACKNOWLEDGMENTS

The author gratefully acknowledges helpful discussions with Ulf Sandberg. Initial stages of this work were completed at the Yukawa Institute of Theoretical Physics, Kyoto University, Japan, with the support of the Japan Society for the Promotion of Science and the Japanese Ministry of Education, Science and Culture (Mombusho).

[1] M. Heckl, ''Tyre noise generation,'' Wear **113**, 157–170 (1986).
[2] R. E. Hayden, ''Roadside noise from the interaction of a rolling tire with road surface,'' in *Proceedings of the Purdue Noise Conference*, West Lafayette, IN, 1971, pp. 62–67.
[3] K. Plotkin, W. Fuller, and M. Montroll, ''Identification of tire noise generation mechanisms using a roadwheel facility,'' in *International Tire/Road Noise Conference 1979*, pp. 127–141.
[4] I. D. Wilken, L. J. Oswald, and R. Kickling, ''Research on individual noise source mechanisms of truck tires: Aeroacoustic sources,'' in *SAE Highway Noise Symposium* (Society of Automobile Engineers, Warrendale, 1976), 762022, pp. 155–165.
[5] M. G. Richards, ''Cross lug tire noise mechanisms,'' in *SAE Highway Noise Symposium* (Society of Automobile Engineers, Warrendale, 1976), Paper 762024, pp. 181–186.
[6] J. F. Hamet, C. Deffayet, and M. A. Pallas, ''Air-pumping phenomena in road cavities,'' in *International Tire/Road Noise Conference 1990*, pp. 19–29.
[7] J. A. Ejsmont, U. Sandberg, and S. Taryma, ''Influence of tread pattern on tire/road noise,'' in *Transactions of the Society of Automotive Engineers* (Society of Automotive Engineers, Warrendale, 1984), pp. 1–9.
[8] M. Jennewein and M. Bergmann, ''Investigations concerning tyre/road noise sources and possibilities of noise reduction,'' Proc. Inst. Mech. Eng., Part C: Mech. Eng. Sci. **199**, 199–205 (1985).
[9] N.-A. Nilsson, ''Air resonant and vibrational radiation—possible mechanisms for noise from cross-bar tires,'' in *International Tire/Road Noise Conference 1979*, pp. 93–109.
[10] U. Sandberg and G. Descornet, ''Road surface influence on tire/road noise,'' in *Proceedings of Internoise 1980: Noise Control Foundation*, 1980, pp. 1–14.
[11] M. C. Bérengier, M. R. Stinson, G. A. Daigle, and J. F. Hamet, ''Porous road pavements: Acoustical characterization and propagation effects,'' J. Acoust. Soc. Am. **101**, 155–162 (1997).
[12] J. M. Cuschieri, S. Gregory, and M. Tournour, ''Open grid bridge noise from grid and tire vibrations,'' J. Sound Vib. **190(3)**, 317–343 (1996).
[13] W. Kropp, ''Structure-borne sound on a smooth tyre,'' Appl. Acoust. **26**, 181–192 (1989).
[14] O. A. Olatunbosun and J. W. Dunn, ''Generalized representation of the low frequency radial dynamic parameters of rolling tyres,'' Int. J. Vehicle Design **12**, 513–525 (1991).
[15] S. C. Huang, ''The vibration of rolling tyres in ground contact,'' Int. J. Vehicle Design, **13**(1), 78–95 (1992).
[16] U. Sandberg, ''Road traffic noise: The influence of the road surface and its characterization,'' Appl. Acoust. **21**, 97–118 (1987).
[17] M. J. Zucrow and J. D. Hoffman, *Gas Dynamics* (Wiley, New York, 1976).
[18] Z. U. A. Warsi, *Fluid Dynamics: Theoretical and Computational Approaches* (CRC, Boca Raton, 1993).
[19] K. A. Hoffmann and S. T. Chiang, *Computational Fluid Dynamics for Engineers* (Engineering Education System, Wichita, KS, 1993).
[20] J. D. Anderson, *Computational Fluid Dynamics: The Basics with Applications* (McGraw–Hill, New York, 1995).
[21] P. M. Morse and K. Uno Ingard, *Theoretical Acoustics* (McGraw–Hill, New York, 1968).
[22] S. J. Elliott, ''Active control of structure-borne noise,'' J. Sound Vib. **177**(5), 651–673 (1994).
[23] S. Weinberg, *Gravitation and Cosmology: Principles and Applications of the General Theory of Relativity* (Wiley, New York, 1972).
[24] M. J. Gagen, ''Expelled jets from squeezed fluid singularities,'' accepted by AIAA J.
[25] R. W. MacCormack, ''The effect of viscosity in hyper-velocity impact cratering,'' AIAA Paper, 69–354 (1969).